Soft Matter

Accepted Manuscript

ROYAL SOCIETY OF CHEMISTRY

www.rsc.org/softmatter

Table of Contents (TOC)

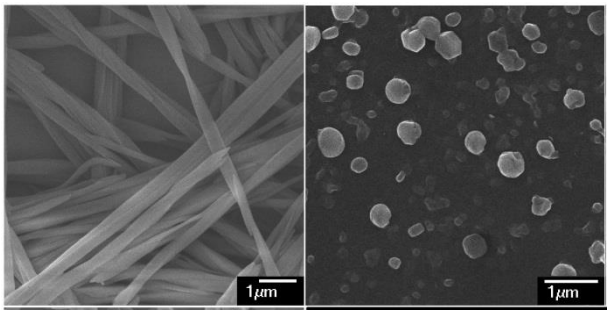

Different morphologies from fiber structures to nanoparticles can be manipulated by different ultrasound treatment.

Soft Matter

RSCPublishing

ARTICLE

Ultrasound-induced controllable morphology and growth dimension in a Dihydrazide-Based self-assembly system

Cite this: DOI: 10.1039/x0xx00000x

Received ooth January 2012,
Accepted ooth January 2012

DOI: 10.1039/x0xx00000x

www.rsc.org/

Yan Zhang, Hao Ding, Yangfang Wu, Chunxue Zhang, Binglian Bai, Haitao Wang* and Min Li*

We have demonstrated ultrasound-induced organogels based on twin-tapered dihydrazide derivatives, oxalyl acid N, N-di (3, 4, 5-trialkoxybenzoyl)-hydrazide (FH-Tn). Ultrasound irradiation has proved to influence gel properties at micro-levels. Different self-assembled structures from entangle fibers, to tube-like structures and nanoparticles can be easily manipulated by tuning irradiation time and water bath temperature. FT-IR spectra exhibit weakened hydrogen bonding interactions, and XRD studies showed different packing modes before and after sonication. In addition, ultrasound can have effects on gel properties at macro-levels. Gel obtained from ultrasound treatment possesses different wetting properties, relatively worse rheological properties and thermo-stability. Kinetic studies based on dynamic fluorescence spectra, rheological studies and theoretical calculations suggest that molecular aggregation mode differed from one-dimension to two-dimension for the gel after sonication.

Introduction

In recent years, stimuli-responsive gelation has been the subject of an increasing interest due to its potential applications in template materials,[1] sensors,[2] actuators, [3]shape memories,[4] and gene delivery devices.[5] Weak non-covalent interactions, such as hydrogen bonding, π-π stacking, donor–acceptor interactions and/or van der Waals interactions[6] are mainly responsible for the self-assembly of low-molecular-weight organic gelators (LMOGs) to form three-dimensional network.[7] While external stimuli, such as temperature,[8] pH[9] and UV/visible light,[10] may bring some changes in the chemical structure, molecular configuration or self-assembly process of the gelator.

Very recently, ultrasound, a novel method to influence self-assembly process and control the functionality of materials, [11]has incorporated into the list. Although the fact that ultrasound can induce chemical reactions in polymers has been known since the 1930s,[12] it is really hard to believe that ultrasound, which is generally used to destroy weak intermolecular interactions, could induce gel formation until Naota and associates reported the first example of ultrasound-induced gelation based on a coordination compound in 2005.[13] From then on, ultrasound was used as an effective method to affect the original hydrogen bonding and π-π stacking interactions, and then re-organize the morphologies.[14] Xiangyang Liu observed an ultrasound-induced structural transformation from separate spherulites in solution to three-dimensional fibrillar network in a hydrogen bond-assisted gelator, *N*-lauryl-$_L$-glutamic acid di-n-butylamide.[15] Jiannian Yao described an induced gelation and unique self-assembled morphologies due to changes from intra- to intermolecular hydrogen-bonding by ultrasound.[16] Tao Yi and co-workers designed and synthesized a novel gelator, which could change morphologies between a three dimensional gel network and vesicles through ultrasound treatment within a certain concentration range.[17] In another paper, they introduced a chiral amino acid into an existing ultrasound-responsive gelator, and the new compound turned out to be responsive to ultrasound.[18] At the same time the position of the amino acid played a crucial role in tuning the sonication properties of the gelators. A series of binuclear platinum complexes, whose emission intensity from gels could be controlled by changing sonication time, linker length, and optical activity, had been synthesized by Naota and his fellows.[19]

Although a large amount of efforts have been paid to the molecular design, synthesis of the LOMGs capable to respond to ultrasound, few of them focus on finding suitable conditions, such as ultrasound power, temperature and ultrasound irradiation time, to obtain some successes in getting a deeper understanding on the responsive mechanism and getting more useful structures. On this account, we mainly highlighted the effects of environmental aspects, water bath temperature and

ultrasound time, on the aggregation behaviours and properties of the resultant gels.

In consideration of gelators with hydrogen bonding interactions may be prone to be sonication-sensitive, in this work we choose the twin-tapered derivatives, oxalyl acid *N, N*-di(3,4,5-trialkoxybenzoyl)-hydrazide (FH-Tn, Scheme 1),[20] which may generate multiple hydrogen bonds, as the gelator. To the best of our knowledge, this is the first example related to ultrasound-induced morphology and property changes due to changes of environmental parameters and this study also open a door for the development of responsive soft materials. Moreover, kinetics of the ultrasound-induced gel formation were also explored in this article, since it could give plenty of information about the sol-gel process and the fractal dimension (D_f) obtained could provide direct information about the gel structures.[21]

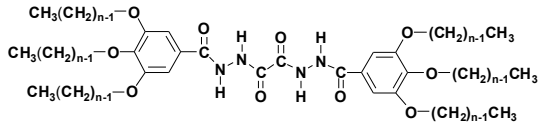

Scheme 1 Molecular structure of FH-Tn (n=5, 6)

Results and discussion

Effects of sonication on the gel properties

As reported in our previous work, [20] both FH-T5 and FH-T6 showed strong gelation ability only in ethanol, although slowly, in a traditional heating-cooling process (designated as T-gel, shown in Figure 1). But we found that irradiation of homogeneous solution of both FH-T5 and FH-T6 in ethanol with ultrasound waves (100 W, 40 kHz) gave a stable gel (designated as S-gel) after several minutes (designated as *ts*) in a 50 ℃ water bath (designated as *Tw*). However, no gelation was observed from them upon ultrasound irradiation in other solvents.

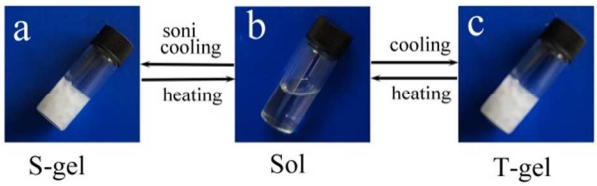

Figure 1 Reversible gelation of FH-T6 in ethanol (6.3 mg/mL): a, S-gel after pre-sonication; b, solution before gelation; c, T-gel after a heating-cooling process. The complete photos are shown in supplementary information (Figure S1).

Critical gelation concentration

Sonication could promote gel formation at relatively low concentration: the critical gelation concentration (CGC) of FH-T5 in ethanol was decreased from 4.8×10^{-3} mol/L in the cooling process to 2.9×10^{-3} mol/L in the ultrasound process (5 min, 50 ℃). For the case of FH-T6 gel, the CGC varied from 2.1×10^{-3} mol/L to 1.6×10^{-3} mol/L (5 min, 50 ℃).

Gelation rate

In addition, sonication could also accelerate gelation speed in a large extent. For example, molecules of FH-T6 were observed to form stable gel in ethanol after several hours by a typical heating–cooling process. However, after irradiation for about 5 min (*Tw*=50 ℃), stable gel was observed to form in half an hour.

Thermal stability

To assess the stability of the two gels in a simple way, gel-sol transition temperature (T_{gel}) was measured with the so-called "inverted test tube" method.[22] Figure 2 showed the T_{gel} of both T-gel and S-gel as a function of concentration. As the molar concentration of the gelator increased, T_{gel} increased nonlinearly, until a relative steady value. Nevertheless, among the tested concentration range, T-gels had higher T_{gel} values than those of S-gels at the same concentration. Actually, T_{gel} value was more like the temperature at which the solvent molecules came out of gel networks, which was an indication of the strong network morphology. This result demonstrated that T-gel was more stable than S-gel upon thermal condition, under the same concentration.

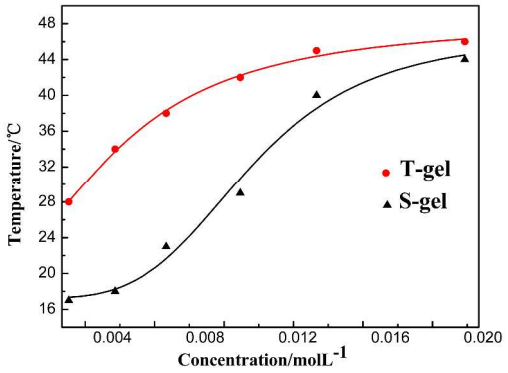

Figure 2 the change of gel-sol phase transition temperature, T_{gel} with respect to concentration of S-gel (*ts*=5 min, *Tw* =50 ℃) and T-gel of FH-T6 in ethanol.

Rheological properties

The linear viscoelastic regimes (LVR) of deformations of the gels were determined by a strain amplitude test ranging from 0.001% to 100% (Figure 3). Afterward, gels were subjected to the frequency sweep test, the storage modulus (*G'*) and the loss modulus (*G''*) of T-gel and S-gel are monitored as a function of applied frequency under a constant strain 0.01%. Rheological results show that both gels have a solid behaviour with the storage modulus exceeding the loss modulus over the entire frequency range.[23] Apart from that, both *G'* and *G''* exhibit a little frequency dependency within the experimental frequency limited, which is owing to the viscoelastic behaviour. Nevertheless, experiments have shown that, in the case of S-gel obtained after 5 min- ultrasound irradiation in 10 and 50 ℃ water bath, the storage modulus was 5380 and 1661 Pa (the value for frequency at 10 Hz, and strain at 0.01%), reduced by 2.6 and 8.5 times, respectively, compared to that of the T-gel (14078 Pa). Furthermore, the yield strains almost stayed

unchanged. These results indicated that the introducing of ultrasound irradiation resulted in a less rigid gel structure.[24] At the same time, the mechanical properties were also influenced by the ultrasonic conditions applied.

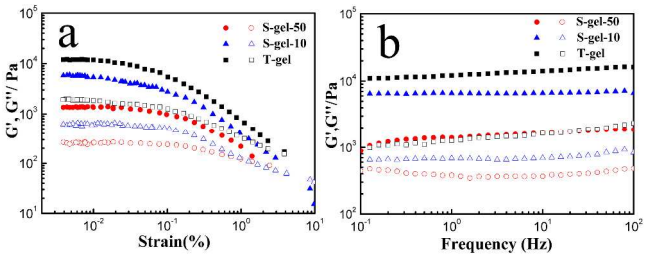

Figure 3: a, Amplitude dependencies of the storage modulus (G') and loss modulus (G'') for FH-T6/ethanol gel samples (4 mg/mL) with and without ultrasound treatment. The frequency is 1Hz; b, Frequency dependency of the storage modulus (G') and loss modulus (G'') for T-gel and S-gel of FH-T6/ethanol (4 mg/mL). The strain amplitude is kept constant at 0.01%. S-gel-10 stands for the gel obtained after 5 min-ultrasound irradiation in 10 ℃ water bath, and S-gel-50 stands for the gel obtained after 5 min-ultrasound irradiation in 50 ℃ water bath

Effects of sonication on the gel morphology

In order to obtain a visual insight into structures of the resultant gels, xerogels of both FH-T6 and FH-T5 obtained from T-gel and S-gel were investigated by SEM.

SEM images of xerogels of FH-T6 with variable *Tw* (*ts*=5 min) were measured, as shown in Figure 4. T-xerogel of FH-T6 exhibited well-defined 3D networks consisting of lots of helical fibres entangled with each other (Figure 4a). The fibres were about 0.2-0.5 μm in width and more than 100 μm in length, suggesting strong directionality in one dimension. It was worth to note that, the fibre structure of a formed T-gel could not be damaged when subjected to ultrasound irradiation, even after 70 min- ultrasound irradiation (Figure S2). 5min-sonication in 0 ℃ ice-water bath brought little morphological change (Figure 4b). While the S-xerogel formed after 5 min-ultrasound irradiation in 10 ℃ water bath, exhibited lots of 1 μm-wide sheet aggregates with rough edges, which were thought to be the adherence of particles to fibres (Figure 4c). If the hot solution was submitted to 5 min-ultrasound irradiation in 35 ℃ water bath, no gel formed. The SEM image showed both long fibres and particles. The width of the fibres was about 1 μm, and the average diameters of the particles were in a range of 0.3 to 1 μm (Figure 4d). Several other data points were also tested (Figure S4), the S-solutions could gel at both 20 and 40 ℃ (weak gel) water baths after 5 min ultrasound treatment and then cooling at room temperature. The S-xerogel showed tube-like structures after 5 min-ultrasound irradiation in 50 ℃ water bath (Figure 4e). The length was usually several microns. Actually, hot solutions at 0 and 10 ℃ water bath had already formed gels within 5 min sonication. For the samples at 35 and 50℃ water bath, the solutions are left at room temperature to form gels after 5 min sonication. Furthermore, repeating the heating–cooling treatment for the ultrasound-induced gel could recover their initial fibre network. Since the fibre structures formed due to an appropriate degree of super-cooling could not be damaged by ultrasound stimulus, it was reasonable to predict that the main effects of ultrasound were to the un-aggregated molecules. In order to prove this assumption, SEM images of S-solution with very low concentration (0.2 mg/mL) were tested. And the results were well consistent with our prediction. As shown in Figure 4f, lots of nanoparticles with diameter ranging from 100 to 500 nm were observed.

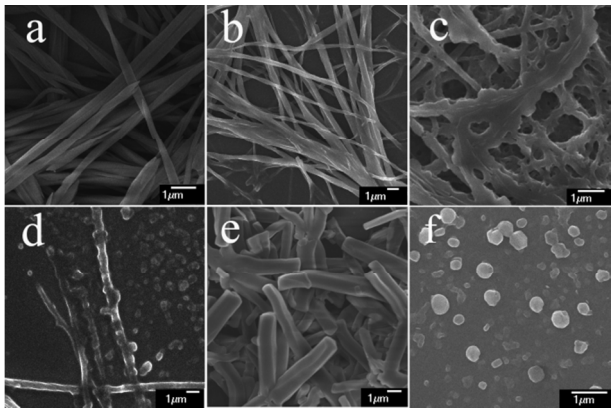

Figure 4 SEM images of dried samples of FH-T6 in ethanol (4mg/mL) a: T-gel (10 ℃ water bath)； b: S-gel (5 min, 0 ℃ ice-water bath); c: S-gel (5 min, 10 ℃ water bath); d: S-solution, can't form gel (5 min, 35 ℃ water bath); e: S-gel (5 min, 50 ℃ water bath),; f: S-solution (0.2 mg/mL, 5 min, 30 ℃ water bath). The complete images are shown in supplementary information (Figure S3).

Similar results can be gained from the images of FH-T5 systems, as shown in Figure 5. Different incubating temperatures yielded different self-assembled morphologies, from fibre morphologies (Figure 5a) of T-gel to rod-like aggregates (Figure 5e) and tube-like (Figure 5f) of S-gel. Furthermore, within a certain temperature range, fibres and rod-like aggregates (or particles) co-existed in the gel system. The content ratio of fibre structures decreased gradually with the increase of *Tw*. FH-T5 formed S-gels at all tested temperatures, including 35 °C, possibly due to the stronger gelation ability than FH-T6.

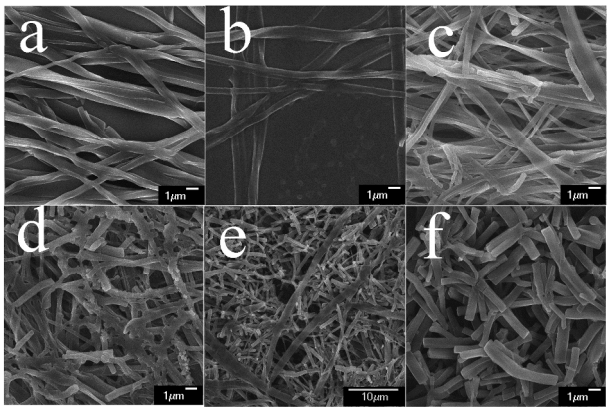

Figure 5 SEM spectra of xerogels of FH-T5 in ethanol (4mg/mL) a: T-gel (3 ℃ water bath)； b: S-gel (5 min, 0 ℃ ice-water bath); c: S-gel (5 min, 25 ℃ water bath); d: S-gel, (5 min, 35 ℃ water bath); e: S-gel (5 min, 45 ℃ water bath); f: S-gel (5 min, 60 ℃ water bath), the complete image is shown in supplementary information (Figure S5).

The individual influence of *Tw* without ultrasound irradiation in typical heating-cooling fashion and similar fashion as S-gels, only eliminating the sonication procedure, on the morphologies was also tested. As shown in Figure 6, the solution couldn't form gel in this fashion. Only short fibres were visible in the monitor area. So it was reasonable to indicate that the morphological differences were owing to the combined effects of *Tw* and irradiation time.

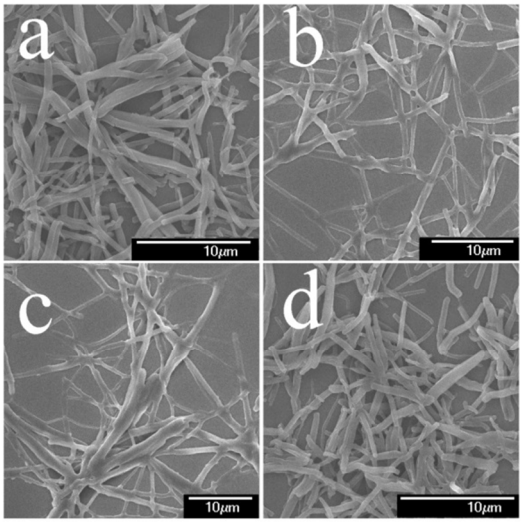

Figure 6 SEM images of dried samples of FH-T6 in ethanol (4mg/mL) after a: 5 min in 0 ℃ ice-water bath; b: 5 min in 10 ℃water bath; c: 5 min in 35 ℃ water bath; d: 5 min in 50 ℃ water bath, and left at room temperature (only for c and d).

In the above experiments, we merely changed water bath temperature. In order to examine the effects of irradiation time during the assembled process, we studied SEM images with different irradiation time.

As shown in Figure 7a, the S-xerogel (*ts*=1 min, *Tw*=10℃) showed almost the same fibrillar morphology as that of the T-xerogel (Figure 4a). When *ts* evaluated to 3 min, particles began to appear in the monitor area (Figure 7b). While lots of 1 μm-wide sheet aggregates with rough edge (Figure 7c) were observed when *ts* evaluated to 5 min. Longer irradiation time would bring no damage to the formed structures, as shown in Figure S6. These results indicated that irradiation time had little effects on the formed fibre morphologies but played an important role in determining the amount of particle aggregates. And once the structures of S-gel formed, additional time would have little benefits on the morphologies. Similar results could be gained from the images obtained from FH-T5 systems, as shown in Figure S7.

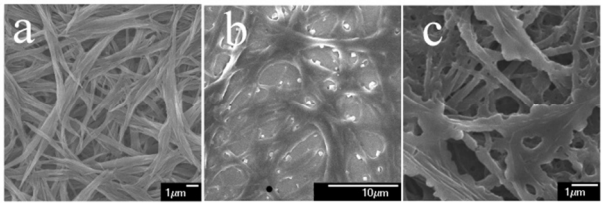

Figure 7 SEM images of S-samples after sonication for a, 1 min, b, 3 min, c, 5 min of FH-T6/ethanol in 10 ℃ water bath (4 mg/mL), and then cooled at 10 ℃ to form gel.

In view of different topological structures in gel network and important roles of morphological changes played in determining macroscopic properties, the very acts of different thermal stability and mechanical stability could be easily explained. Obviously, fiber entanglements in T-gel could trap more solvent and make flow more difficult, which resulted in a more stable gel structure upon thermal and mechanical stimulus. While nanoparticles or tube-like structures made it difficult to immolize solvent when subjected to external stimulus, resulting in a less stable gel network.

Effects of sonication on the surface wettability

Taking these various nano- and micro-structures into consideration, the wetting properties of films of xerogels were investigated. As shown in Figure 8a, the static contact angle (CA) of water on the film of T-xerogel was measured to be 122.1°. While the film of the xerogel, obtained after a brief ultrasound irradiation in 35 ℃ water bath, which showed both fibres and nanoparticles, had a static contact angle of 146.7 °(Figure 8b), even though they were formed by the same chemical structure. Furthermore, the contact angle of the S-xerogel (5 min, 60 ℃) decreased to 111.2° (Figure 8c), possibly owing to the absence of nanoparticles. In a word, the surface wettability could be simply manipulated by additional use of ultrasound irradiation.

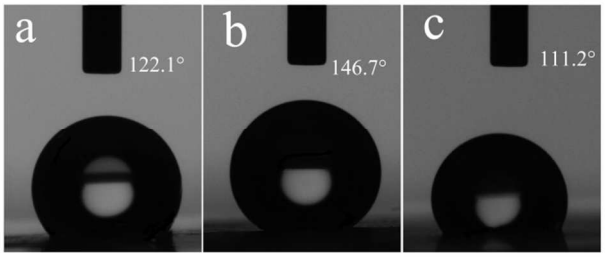

Figure 8 photographs of water droplets on silicon slides coated with FH-T5 xerogels, a: T-gel; b: S-gel (5 min, 35 ℃); c: S-gel (5 min, 60 ℃). All contact angles were analysed by using Laplace–Young Fitting.

FT-IR Spectroscopy

To obtain the insight into the gelation mechanism, FT-IR spectra of xerogels of T-gel and S-gel were measured. A comparison of the FT-IR spectra of FH-T6 xerogels was shown in Figure 9 and Table 1. For T-gel, the presence of N-H stretching bands at 3185 cm^{-1}, three relatively weak C=O stretching bands at 1677, 1658 and1610 cm^{-1},indicated that the N-H groups are associated with C=O groups via strong hydrogen bonding interactions.[25] The appearance of $\nu as (CH_2)$ and $\nu s (CH_2)$ bands at 2928 cm^{-1} and 2853 cm^{-1} indicated disordered alkyl chains.[26] For the S-gel (*ts*=5 min, *Tw*=10 ℃), the hydrogen-bonded N-H stretching peak was observed at higher wavenumber (3193 cm^{-1}) than that of T-gel (3185 cm^{-1}), red-shifted about 8 cm^{-1}. At the same time, ν(C=O) moved to

1694, 1658 and1611 cm^{-1}, which suggested a weaker hydrogen bonding interaction than T-gel. Furthermore, for the IR spectrum of the gel after 5 min-ultrasound in 50 ℃water bath, red-shift of N-H stretching peak to 3204 cm^{-1}, and C=O stretching peak to1694, 1671 and1611 cm^{-1}, indicated the weakest hydrogen bonding interaction of the three. Meanwhile, the deformation vibrations of CH_2 also shifted from 1468 and 1443 cm^{-1}in T-gel to 1466 and 1428 cm^{-1}in S-gel, indicating a more ordered conformation during self-assembly process. Similar conclusion could be drawn by comparison the results of the xerogels of FH-T5, as shown in Figure S8. From this aspect, it suggested that ultrasound treatment did have some effects on changing molecular conformation and weakening molecular hydrogen bonding interaction during the self-assembly process.

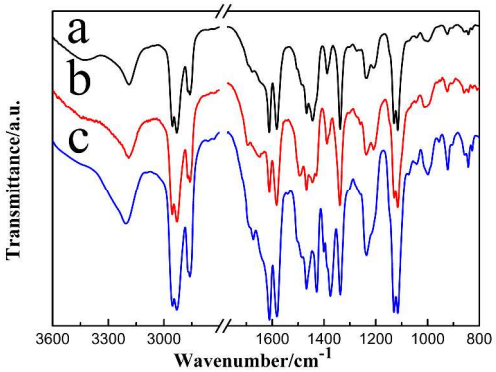

Figure 9: FT-IR spectra of a: T-xerogel of FH-T6/ethanol （4 mg/mL）, S-xerogel of FH-T6/ethanol （4 mg/mL）after 5 min-ultrasound in b: 10 ℃ water bath; c: 50 ℃ water bath.

Table 1 Assignments of infrared frequencies for FH-T6 samples

Assignments	IR frequency (cm^{-1})		
	T-gel	S-gel-10	S-gel-50
ν (N-H)	3185	3193	3204
ν (C=O)	1677,1658,1610	1694,1658,1611	1694,1671,1611
δ(CH2)	1468,1443	1466,1428	1466,1428

Effect of sonication on packing modes in xerogels

In order to clarify if there were any changes in molecular packing modes of the gels after ultrasound irradiation, X-ray diffraction patterns of both T-xerogels and S-xerogels (*ts*=5 min) were measured and the results are shown in Figure 10 and Table 2. The XRD pattern of the xerogels showed many sharp peaks at both lower and higher angle ranges, indicating crystalline features and high ordered structures in gel state. The XRD profile of the T-xerogel (Figure 10a) showed main peaks at 3.3°, 4.7°, 6.0°, 8.6° and 10.2°(2θ values), corresponding to *d* values of 26.61, 18.91, 14.67, 10.27 and 8.68 Å, respectively, indicating a triclinic structure of the aggregates within the gel. The XRD profile of the S-xerogel (*Tw*=50 ℃, Figure 10d) was similar to that of the T-xerogel, indicating a similar packing modes. While, for XRD patterns of xerogels formed in 10 ℃ and 35 ℃ water bath, the occurrence of three new peaks corresponding to d-spacing of 23.63 (2, 0, 0), 19.70 (2, 0, -2), 14.80(3,1,0) and 13.08 Å (1, 1, 2), indicated the presence of a monoclinic packing mode. These peaks were more highlighted in samples prepared in higher *Tw* condition. Semi-quantitative analysis showed approximately 37% and 65% monoclinic content for samples formed in 10 ℃ and 35 ℃ conditions, respectively. When compared with SEM images, triclinic packing mode could be easily attached to fiber and tube-like aggregates, while monoclinic packing mode to particle aggregates. A similar XRD result was gained for the FH-T5 xerogels, shown in Figure S10. New peaks attached to particle aggregates were only observed in samples formed after 5 min ultrasound irradiation in water temperature below 35 ℃.

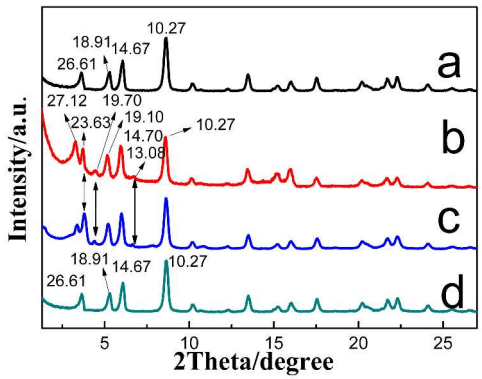

Figure 10 XRD patterns of a: T-xerogel; and S-xerogel formed after 5 min ultrasound irradiation in b:10 ℃, c: 35 ℃, d: 50 ℃, water bath of FH-T6 in ethanol (4 mg/mL).

Table 2 XRD data*

Patterns a and d			Patterns b and c		
Phase	d(Å)	Miller	Phase	d(Å)	Miller
	26.61	(0,0,1)		27.12	(0,0,1)
	18.91	(0,-1,1)		*23.63*	*(2,0,0)*
Triclinic	14.67	(-1,1,0)	Triclinic	*19.70*	*(2,0,-2)*
	10.27	(0,-2,1)		19.10	(0,-1,1)
	8.68	(1,-2,2)	*Monoclinic*	14.70	(-1,-1,0)
	8.30	(2,-1,1)			*(3,1,0)*
	7.23	(-1,-1,4)		*13.08*	*(1,1,2)*
	6.57	(-1,-2,4)		10.27	(0,-2,1)
	5.82	(-1,-1,5)		8.71	(1,-2,2)
	5.5	(0,-2,5)		8.33	(2,-1,1)

*Data reduction and phase identification were done by using MDI JADE 5.0 with PDF 2004 database. Card No. of the reference patterns are 83-0605 (Triclinic) and 46-1756 (Monoclinic).

The above results demonstrated that introducing of ultrasound irradiation did not damage the original packing modes of the molecules in gel phase. Indeed, the effect of ultrasound irradiation was to promote new packing via inducing aggregation of the molecules which are initially soluble in solvent.

Kinetics of gelation

To explain the formation of the different morphologies induced by ultrasound treatment, kinetics of gel formation of FH-T5 and FH-T6 in ethanol had been investigated by fluorescence and rheology methods. The results of FH-T5 were shown in Figure S11 and Figure S12.

Both FH-T6 and FH-T5 showed strong emission in gel state although they were non-emissive in ethanol (called an aggregation-induced emission—AIE gelation process), as shown in Figure S13 and Figure S14. This was the foundation of kinetic studies of gelation process through monitoring fluorescence intensity changes. Below, intensity changes (λ_{ex}=270 nm, λ_{em} =380 nm) of FH-T6 in ethanol during self-assemble process were studied in detail.

As shown in Figure 11a, the curve at the early stage of gelation showed a little deviation from the straight line, and then, fluorescence emission intensity increased drastically until a maximum value was reached. The changes indicated that the fibrillation of FH-T6 in ethanol during gelation was autocatalytic, following a nucleation process.[27] The time that intensity began to increase rapidly was thought as gelation time-t_g, and the time at which the maximum intensity reached was thought as the accomplishment of gelation. As shown in Figure 11, the velocity of gelation was dependent on sonication time. For the same gelator concentration and water bath temperature, the longer sonication time, the shorter gelation time results: gel occurred at 371 min for the typical heating-cooling system, while only 27 min for the system subjected to sonication for 5 min. In other words, ultrasound irradiation could induce a more effective gelation process, namely favored the aggregation. This might be due to the extreme high heating and cooling rates, as well as intense heating and pressure environments generated by the cavitation effects.[28]

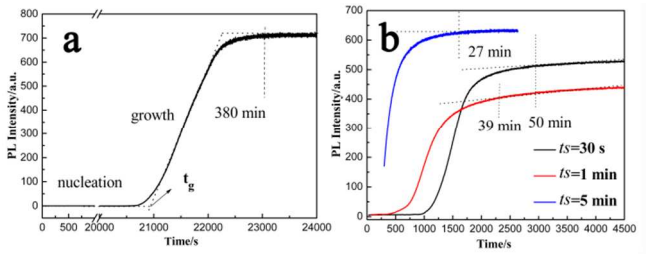

Figure 11 Time-dependent fluorescence spectra of FH-T6 (6 mg/mL) in ethanol a: at 10 ℃, b: after different sonication time (*ts*) at 50 ℃ water bath, and then cooled at 10 ℃. Excited wavelength λex=270 nm, λem =380 nm.

Avrami equation (eq.2), and modified equation (eq.3),[29] which were initially used to describe the crystallization of polymer melts,[30] were used to further analyse the data obtained, since the well crystalline properties of FH-T6 in ethanol according to the XRD results.

$$\ln\left[1-X_g(t)\right] = -kt^{D_f} \qquad \text{eq. 2}$$

$$\ln[-\ln\frac{X(\infty)-X(t)}{X(\infty)-X(0)}] = D_f \ln k + D_f \ln t \qquad \text{eq. 3}$$

As applied to gels, k is a temperature-dependent parameter like a rate constant, D_f is the so-called fractal dimension which is commonly used to describe the branches complexity of the molecules, and also reflect the type of organization during self-assembly.[31] $Xg(t)$ is the volume fraction of the gel phase which is measured as a function of time: by fluorescence, the increase of emission intensity at 380 nm with excitation at 270 nm; by rheology, the increase of storage modulus G'. Zero-time is defined as when X starts to increase rapidly from its initial value.

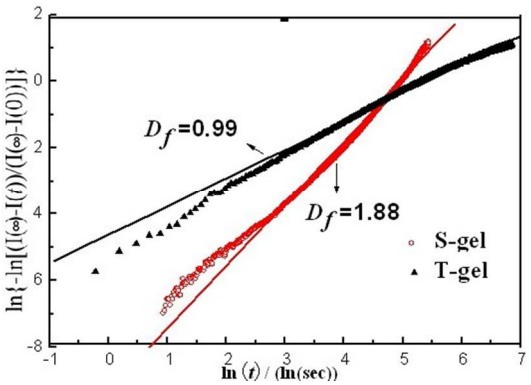

Figure 12: Avrami plot of the fluorescence data of T-gel and S-gel (5 min-ultrasound irradiation in 50 ℃ water bath) for FH-T6 in ethanol (4 mg/mL).

Figure 12 showed Avrami plots based on kinetic FL data of T-gel and S-gel. It was observed that S-gel had larger fractal value than that of T-gel. For T-gel, D_f was 0.99, indicating a linear one dimension growth. And this was well consistent with the long fibres observed from SEM photos. However, for S-gel (Tw=50℃, ts=5 min) consisting of short tubes, D_f was 1.88, indicating a two-dimensional growth pattern.[32]

In consideration of the operation of pre-sonication and time-dependent rheological experiments were impossible at the same time, dynamic rheological data were merely collected for FH-T6/ethanol under non-ultrasound condition. As seen in Figure 13a, both G' and G'' were very small at the early time, indicating a low viscosity liquid. Thereafter, both G' and G'' increased until a plateau value. And the equilibrium G' value was much larger than G''. Upon treating the data according to Avrami equation, fractal dimension D_f of T-gel was 1.15, a little bigger than 0.99 obtained from fluorescence results. These results illustrated that during self–assemble process of FH-T6/ethanol T-gel, fibres formed in a one-dimensional aggregation mode once again.

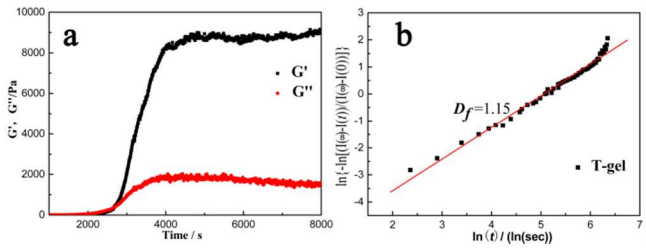

Figure 13 a, Rheological time sweep experiment for FH-T6/ethanol T-gel sample (4 mg/mL). The frequency is 1 Hz and the strain is 0.01%; b, Avrami plot of rheological data of figure 10a.

All the results above demonstrated that ultrasound irradiation played an important role in the formation of new aggregates. It was reasonable to predict that morphological differences are mainly due to a combined effect of thermal nucleation and ultrasonic nucleation processes. For the non-ultrasonic samples, when hot solution was put into the water bath, part of the molecules would tend to self-assemble into fibres due to thermal nucleation process. The other part would still solute in the liquid phase. By applying sonication, thermal nucleation and ultrasonic nucleation co-existed during the self-assembly process. The part of soluble molecules would be trapped in an extreme high heating and cooling rates conditions promoted by cavitation effect and then self-assembled to form nanoparticles due to ultrasonic nucleation process. So fibres and particles would co-exist in the system. The further aggregation of the original soluble molecules made the system much easier to form gel, resulting in a decrease of CGC. With *Tw* increasing, more molecules would tend to be molecular dispersed, resulting in the formation of more nanoparticles or tube-like morphologies. When the temperature was low, there would be more fibres in the system, and the fibres interconnected with each other to form a stable gel. However, during a certain temperature range, the small amount of fibres and large amount of particles were not able to immobilized solvent. This was the reason that solution after sonication at 35 ℃ could not form gel. When *Tw* was beyond a certain value, only tube-like structures formed due to the insufficient degree of super-cooling to form fibre aggregates. And the tube-like aggregates also had the ability to immobilize solvent from flowing. So different aggregation morphologies, ranging from entangled fibres, tube-like structures to nanoparticles could be simply manipulated by changing *Tw* and sonication time applied. A gel with different topological structures would present different properties, such as thermal stability, surface wettability and mechanical stability. Furthermore, the S-gel can change back to the original T-gel by applying a heating-cooling process, thus, the process can be used as a switch in the structure tuned by heat and ultrasound.

Experimental

The gelator FH-T5 and FH-T6 were synthesised as described elsewhere.[20]All chemicals were Laboratory reagent grade and used without further purification.

Organogel was prepared by mixing a predetermined amount of FH-T6 (or FH-T5) with solvent in a sample vial with a crew cap and heated until the solids were completely dissolved (about 105 ℃). The solution was allowed to cool to room temperature. Gelation was considered to occur when the test tube can be turned upside down without fluid. For all ultrasound samples, ultrasound treatments were used just after heating the mixture fully dissolved and before cooling the hot solution at room temperature by using the laboratory use of ultrasound glassware cleaner that has a temperature-controllable water bath (100 W, 40 kHz).

For the inverted tube gel melting experiments, gels at a series of concentrations ranging from $2x10^{-3}$ to $2x10^{-2}$ mol/L were prepared in test tubes and put upside down in a thermostat water bath with the temperature raised slowly. It is worth to note that the upside down test tubes were sealed using para-film. The temperature at which the last tiny part of gel was completely dissolved was identified as the gel melting temperature (T_{gel}).

Scanning electron microscopy (SEM) observations were recorded with a SSX-550 apparatus. Samples for this measurement were prepared by casting the organogel on silica substrate. For the observation of the solution samples after ultrasound treatment, a drop of solution was cast onto silica substrate. All the samples were dried at room temperature overnight, and then coated by gold before observation.

Surface wettability was characterized using a commercial video-based, software-controlled contact angle analyzer (Kruss DSA 30) on the xerogel film at room temperature. The water droplet size used for measurements was 20 μL. At least five different positions were measured and averaged to get a reliable value for the same sample.

FT-IR spectra were recorded with a Perkin – Elmer spectrometer (Spectrum One B). The samples were pressed tablets with KBr. X-Ray diffraction was carried out with a Bruker Avance D8 X-ray diffractometer. Data reduction and phase identification were done by using MDI JADE 5.0 with PDF 2004 database.

The rheological properties were performed on a TA instrument (AR2000 Rheometer) equipped with a stainless steel plate of 40 mm diameter. The samples were sandwiched between the two plates with a gap of 0.5 mm throughout the experiments. The frequency sweep experiments were carried out at a constant strain, well within the linear visco-elastic region. To minimize dehydration, a trap was employed.

The fluorescence measurements were performed using a Perkin Elmer LS 55 fluorescence spectrophotometer with a 1.0 cm length quartz cell. The emission intensity was 380 nm and the excitation intensity was 270 nm. UV-vis absorption spectra were recorded on a Shimadzu UV-2550 spectrometer.

Conclusions

In conclusion, effects of ultrasound irradiation on organogels developed from twin-tapered dihydrazide derivatives (FH-T5, FH-T6) have been systematically investigated. The results suggest that introducing of sonication helps to evaluate gelation ability and accelerate gelation velocity through influencing the self-assembly of the original un-aggregated gelator by the extreme chemical and physical conditions created by acoustic cavitation. Furthermore, ultrasound irradiation time and water bath temperature applied play a crucial role in regulating the molecules orderly and forming new aggregates. SEM images provide evidence of different self-assembled structures from entangle fibers of gel formed through a traditional thermal

nucleation process to tube-like structures and nanoparticles of gels formed through a combined thermal nucleation and ultrasonic nucleation process. The change of growth pattern from one-dimension to two-dimension induced by sonication is also confirmed by kinetic studies. FT-IR and XRD studies exhibit different structural changes before and after sonication. In addition, gel obtained from ultrasound treatment possessed relatively worse rheological properties and thermo-stability due to less entanglement among the assembled structures of the resulting gels. These results may be useful to help to get a deeper understanding of the kinetic of ultrasound-induced aggregation. The reversible sonication triggered gelation and easy manipulated morphologies in ethanol may provide a new way for achieving the application of these soft materials in template area and responsive and shape-memory materials.

Acknowledgements

The authors are grateful to the National Science Foundation Committee of China (Project Nos. 51073071, 21072076 and 51103057), and Project 985-Automotive Engineering of Jilin University for financial support of this work.

Notes and references

*Key Laboratory for Automobile Materials (JLU), Ministry of Education, College of Materials Science and Engineering, Jilin University, Changchun, 130012, P. R. China
E-mail: minli@mail.jlu.edu.cn, haitao_wang@jlu.edu.cn;
Tel: +86 431 85168254
. Electronic Supplementary Information (ESI) available: [details of any supplementary information available should be included here]. See DOI: 10.1039/b000000x/

1. A. Ajayaghosh and S. J. George, *J. Am. Chem. Soc.*, 2001, 123, 5148-5149.
2 A. Matsumoto, R. Yoshida and K. Kataoka, *Biomacromolecules*, 2004, 5, 1038-1045.
3 H. Suzuki, J. *Intell. Mater. Syst. Struct.*, 2006, 17, 1091-1097.
4 H. Goto, H. Q. Zhang and E. Yashima, *J. Am. Chem. Soc.*, 2003, 125, 2516-2523; Y. Li, Z. B. Hu and Y. Y. Chen, *J. Appl. Polym. Sci.*,1997, 63, 1173-1178.
5 J. Chatterjee, Y. Haik and C. J. Chen, *Colloid Polym. Sci.*, 2003, 281, 892-896; J. F. Mano, *Adv. Eng. Mater.*, 2008, 10, 515-527.
6 N. Amanokura, K. Yoza, H. Shinkai and D. N. Reinhoudt , *J. Chem. Soc.*, Perkin Trans. 2,1998, 2585-2591; K. Hanabusa, Y. Maesaka and H. Shirai, *Tetrahedron Letters*, 40, 1999,2385-2388.
7 N. M.Sangeetha and U. Maitra, *Chem. Soc. Rev.*, 2005,34, 821-836; P. Jonkheijm, P. van der Schoot, A. P. H. J. Schenning and E. W. Meijer, *Science*, 2006, 313, 80-83.
8 S. I. Kawano, N. Fujita and S. Shinkai, *Chem. Eur. J.* , 2005, 11, 4735-4742.
9 X. Z. Luo, W. G. Miao, S. Wu and Y. Q. Liang, *Langmuir*, 2002, 18, 9611-9612; S. A. Ahmed , X. Sallenave, F. Fages, G. Mieden-Gundert, W. M. Muller, U. Muller, P. Vogtle and J.-L. Pozzo, *Langmuir*, 2002, 18, 7096-7101.
10 K. Murata, M. Aoki, T. Nishi, A. Ikeda and S. Shinkai, *J. Chem. Soc., Chem. Commun.*, 1991, 1715-1718; O. J. Dautel, M. Robitzer, J.-P. Lere-Porte, F. Serein-Spirau and Joël J. E. Moreau, *J. Am. Chem. Soc.*, 2006, 128, 16213-16223.
11 K.Y. Liu, L.Y. Meng, S.L. Mo, M.M. Zhang, Y.Y. Mao, X.H. Cao, C.H. Huang and T. Yi, J. Mater. Chem. C, 2013, 1, 1753–1762; G. Cravotto and P. Cintas, *Chem. Sci.*, 2012, 3, 295–307.
12 Suslick, K. S., *Science*, 1990, 247, 1439-1445.
13 T. Naota and H. Koori, *J. Am. Chem. Soc.*, 2005, 127, 9324-9325.
14 X. D. Yu, L.M. Chen, M.M. Zhang and T.Yi, *Chem. Soc. Rev.,* 2014, 43, 5346-5371.
15 R. Y. Wang, X. Y. Liu and J. L. Li, *Cryst. Growth Des.*, 2009, 9, 3286-3291.
16 Y. B. Wang, C.L. Zhan, H.B. Fu, X. Li, X.H. Sheng, Y.S. Zhao, D.B. Xiao, Y. Ma, J.S. Ma and J.N. Yao, *Langmuir*, 2008, 24,7635-7638.
17 M.M. Zhang, L.Y. Meng, X.H. Cao, M.J. Jiang and T. Yi, *Soft Matter*, 2012, 8, 4494–4498.
18 X. D. Yu, Q. Liu, J. C. Wu, M. Zhang, X. Cao, S. Zhang, Q. Wang, L. Chen and T. Yi, *Chem. Eur. J.*, 2010, 16, 9099-9106.
19 N. Komiya, T. Muraoka, M. Iida, M. Miyanaga, K. Takahashi, and T. Naota, *J. Am. Chem. Soc.*, 2011,133,16054-16061.
20 S. N. Qu, H. T. Wang, Z. X., Yu, B. L. Bai, and M. Li, *New J. Chem.*, 2008, 32, 2023-2029.
21 X. Huang, P. Terech, S. R. Raghavan and R. G. Weiss, *J. Am. Chem. Soc.,* 2006, 128, 15341-15352; M. A. Rogers and A. G. Marangoni, *Langmuir*, 2009, 25, 8556-8566; X. Y. Liu and P. D. Sawant, *Appl. Phys. Lett.*, 2001, 79, 3539-3542.
22 R. G. Weiss and P. Terech., Molecular Gels: Materials with Self-Assembled Fibrillar Networks, Springer, Dordrecht, The Netherlands, 2006.
23 S. K. Samanta, A. Pal, S. Bhattacharya and C. N. R. Rao, *J. Mater. Chem.*, 2010, 20, 6881-6890; A. Pal, B. S. Chhikara, A. Govindaraj, S. Bhattacharya and C. N. R. Rao, J. Mater. Chem., 2008, 18, 2593-2601.
24 M. Avrami, *J. Chem. Phys.,* 1940, 8, 212-224.
25 D. J. Skrovanek , S. E. Howe , P. C. Painter and M. M. Coleman, *Macromolecules*, 1985, 18, 1676-1683.
26 R. A. Macphail, H. L. Strauss, R. G. Snyder and C. A Elliger, J. Phys. Chem.,1984, 88, 334-341; N. V. Venkataraman, S. Vasudevan, YideXu, XinheBao, Xiumei Liu and J. Kuppers, *J. Phys. Chem. B.*, 2001, 105, 1805-1812.
27 G. M. Kavanagh and S. B. Ross-Murphy, *Prog. Polym. Sci.*, 1998, 23, 533-562.
28 G. Cravotto and P. Cintas, *Chem. Soc. Rev.*, 2009, 38, 2684-2697.
29 G. M. Kavanagh and S. B. Ross-Murphy, *Prog. Polym. Sci.*, 1998, 23, 533-562.
30 M. Avrami, *J. Chem. Phys.*, 1940, 8, 212-224.
31 X. Huang, P. Terech, S. R. Raghavan and R. G. Weiss, *J. Am. Chem. Soc.*, 2005, 127, 4336-4344.
32 X. Y. Liu and P. D. Sawant, *Adv. Mater.*, 2002, 14, 421-426.

